

INFLUENCE OF PROJECTION STEPS ON IMAGE QUALITY USING SINGLE SOURCE – SINGLE DETECTOR GAMMA RAY TOMOGRAPH

© 2011 R. Gholipour-Peyvandi, S. Z. Islami-Rad, R. Heshmati, M. Ghannadi-Maragheh

Nuclear Science and Technology Research Institute

AEOI, P.O. Box: 14155-1339, Tehran, Iran

E-mail: rgholipour61@yahoo.com

Received December 30, 2010

The application of the industrial gamma computed tomography (CT) apparatus, using ^{75}Se (148–329 keV) as the gamma source, to evaluate the reconstructed image quality by projection steps is presented. In this article we are intended to focus on influence of view and position variations on reconstructed image quality experimentally. The results show that increasing number of Δr (positions) has inverse and direct relationship with RMS contrast and number of reconstructed image pixels.

1. INTRODUCTION

The goal of industrial gamma ray computed tomography (CT) is to produce internal images of object with sufficient detail to detect important features [1–3]. Computed tomography is a non invasive imaging technique that has been used extensively not only in medicine, but also in nondestructive testing (NDT) for many industrial applications such as mechanical part manufacturing, production of composite materials, waste container inspection, metrology, detection of structural defects in concrete and others, heterogeneities in polymer objects, etc [4–7].

Contrast is usually used to assess the performance of a gamma ray CT [3]. In gamma ray CT, the contrast is affected by several factors. These factors are detector, collimator, counting time, etc. In [8] studied the effect of beam width on reconstructed image contrast. Their results demonstrated that for a constant source collimator aperture, the root mean square (RMS) contrast increases as the detector collimator aperture increases. Also, for a constant detector collimator aperture, the RMS contrast increases as the source collimator apertures increases even though the variation is negligible.

In [9] reported the results of experimental research on rear collimator in gamma ray industrial CT, which plays an important role in suppressing scattered radiation and improving the CT performance. In [10, 11] have investigated the influence of gamma energy on the image contrast for material with different density and counting time and shown that contrast is better in lower energy and higher counting time.

In this article, we are intended to illustrate view and position variations that influence in the contrast and number of reconstructed image pixels. Firstly, the basic theory is defined, and then test setup and experi-

ment condition are explained. Finally, the test outcome is comprehensively discussed and compared.

2. THEORY

Here, we investigate the effect of projection with different views and positions on quality of industrial CT images. Tomography imaging consists of directing γ -rays into an object from multiple orientations and measuring intensity decrease along a series of linear paths. The intensity reduction is characterized by Beer's Law, which describes it as a function of γ -ray energy, path length, and linear attenuation coefficient of material. Finally, an algorithm is used to reconstruct the images [12].

Imaging systems rely on reconstruction of an image from its projections through the process of computed tomography. The number of $\Delta\theta$ and Δr are views (m) and positions (n) respectively, thus positions \times views ($n \times m$) is called projections (Fig. 1). The changes of views and positions can affect on the image quality which here we use two of the image evaluating factors that are root mean square (RMS) contrast and number of reconstructed image pixels.

2.1. RMS contrast

The RMS contrast in each image demonstrates the effect of following factors on image quality. In the reconstructed image, contrast is a criterion which shows the color diversity of images and the difference in visual properties that makes an object (or its representation in an image) distinguishable from other objects and the background. In this paper, RMS contrast was selected to compare image qualities. RMS contrast does not depend on the spatial frequency content or the spatial distribution of contrast in the image. RMS

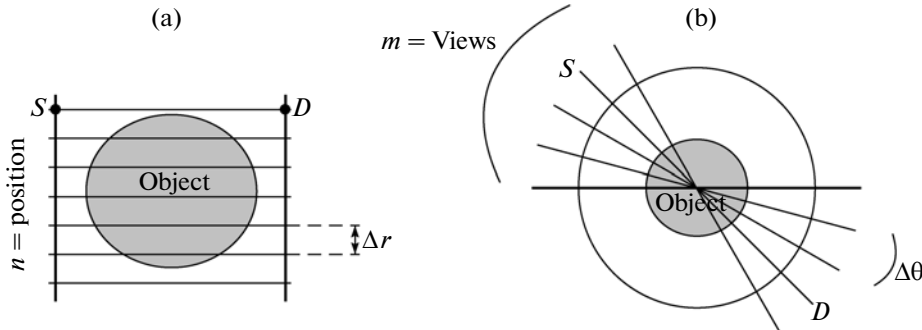


Fig. 1. Describing of (a) position and (b) views. S – Source, D – Detector.

contrast is defined as the standard deviation of the pixel intensities.

$$RMS\ contrast = \sqrt{\frac{1}{MN} \sum_{i=0}^{N-1} \sum_{j=0}^{M-1} (I_{ij} - \bar{I})^2}, \quad (1)$$

where intensities I_{ij} are the i -th and j -th elements of the two dimensional image of size M by N . \bar{I} is the average intensity of all pixel values in the image. The pixels of image I are normalized to have intensity value in the range of (0, 1). For comparing between all reconstructed images with any gamma emitter source, all reconstructed images of energy windows are normalized to intensity range that have most value, in the other words (0, 1) for normalization are related to one window which has most variety in color spectrum. It is particularly necessary to note that these experiments was performed in same condition and are repeatable. As a result, image noise and artifacts do not affect RMS contrast [13, 14].

2.2. Number of Reconstructed Image Pixels

The term resolution is cited as the total number of pixels in the reconstructed image or output pixel. Increasing of this quantity improves image quality [3].

2.3. Radon Transform

The Radon transform computes projections of an image. The Radon transform can be defined as the collection of projections of an object gathered at various angles. In a gamma-ray transmission, I , of a mono-energetic radiation beam traversing a phantom is given by the following equation:

$$g = \ln(I_0/I) = \int_L \mu(x, y) du, \quad (2)$$

where I_0 is the incident beam intensity of the radiation beam, du is some differential path length, $\mu(x, y)$ is the function describing the 2-dimensional distribution of

attenuation coefficient in the imaged object at the point (x, y) , g , the transmittance of the object, is defined as the logarithm of the ratio of the intensity of the detected beam to the intensity of the emitted beam and L is the line along which the beam travels.

The line L can be represented uniquely by the parameters ρ and φ , where φ measures the counterclockwise angle of the line from the vertical, and ρ measures the distance of the line from the origin of the (x, y) plane. Thus, we can use the above formula to define a transform which maps a function $\mu(x, y)$ to a function $g(\rho, \varphi)$, where $g(\rho, \varphi)$ is the line integral of $\mu(x, y)$ over the line defined by ρ and φ . This transform is known as the Radon transform and denoted by R .

The Radon transform of $\mu(x, y)$ at same angle φ is the line integral of μ parallel to the y axis:

$$R_\varphi(x') = \int_{-\infty}^{+\infty} f(x' \cos \varphi - y' \sin \varphi, x' \sin \varphi + y' \cos \varphi) dy'; \quad (3)$$

$$\begin{bmatrix} x' \\ y' \end{bmatrix} = \begin{bmatrix} \cos \varphi & \sin \varphi \\ -\sin \varphi & \cos \varphi \end{bmatrix} \begin{bmatrix} x \\ y \end{bmatrix}. \quad (4)$$

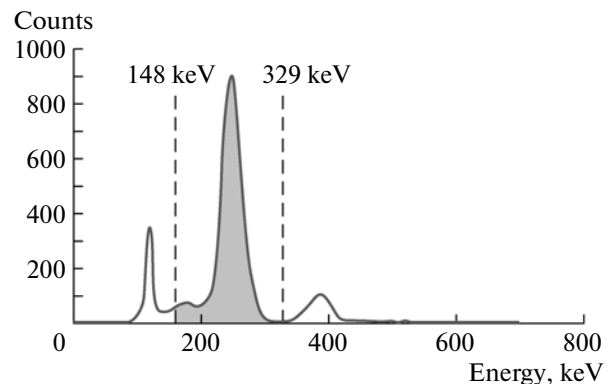


Fig. 2. The energy spectrum for applied source ^{75}Se with energy window 148–329 keV.

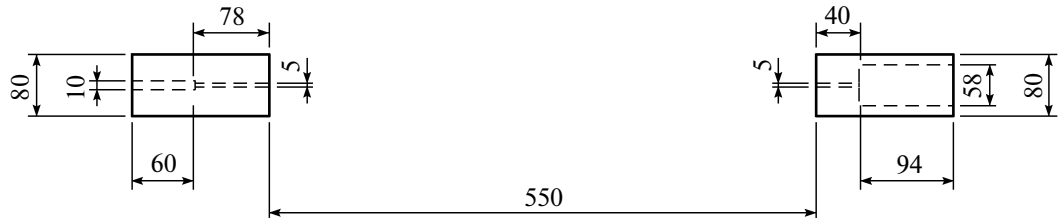


Fig. 3. Configuration of source and detector collimator.

The task of tomographic reconstruction is to find $\mu(x, y)$ given knowledge of $R_\phi(x')$, therefore the Filtered Back Projection algorithm is used to reconstruct from the measured projections the inverse Radon transformation [15–17]. The FBP algorithm begins by filtering the Radon transform data. There are many filters, which can be used in our experiments; we used the Ram-Lak filter to remove some of the high-frequency components that are often fraught with noise.

3. EXPERIMENTAL SET-UP

A single-source – single-detector gamma computed tomography (CT) scanner system was used in this

study. In this setup, a NaI(Tl) detector 5.08 cm in diameter is located opposite the center ^{75}Se (40 mCi) source. The energy window 148–329 keV with the energy spectrum for applied source is shown in Fig. 2. The detector and the source are aligned by a point semiconductor laser; also two cylindrical lead collimators (5 mm diameter) were used for source and detector (Fig. 3).

The position of phantom is defined by three motors, a schematic design of the system hardware is shown in Fig. 4. In each movement, the phantom was rotated by different steps $\Delta\theta$ (m views) and translated in the direction of r with Δr (n positions). The CT

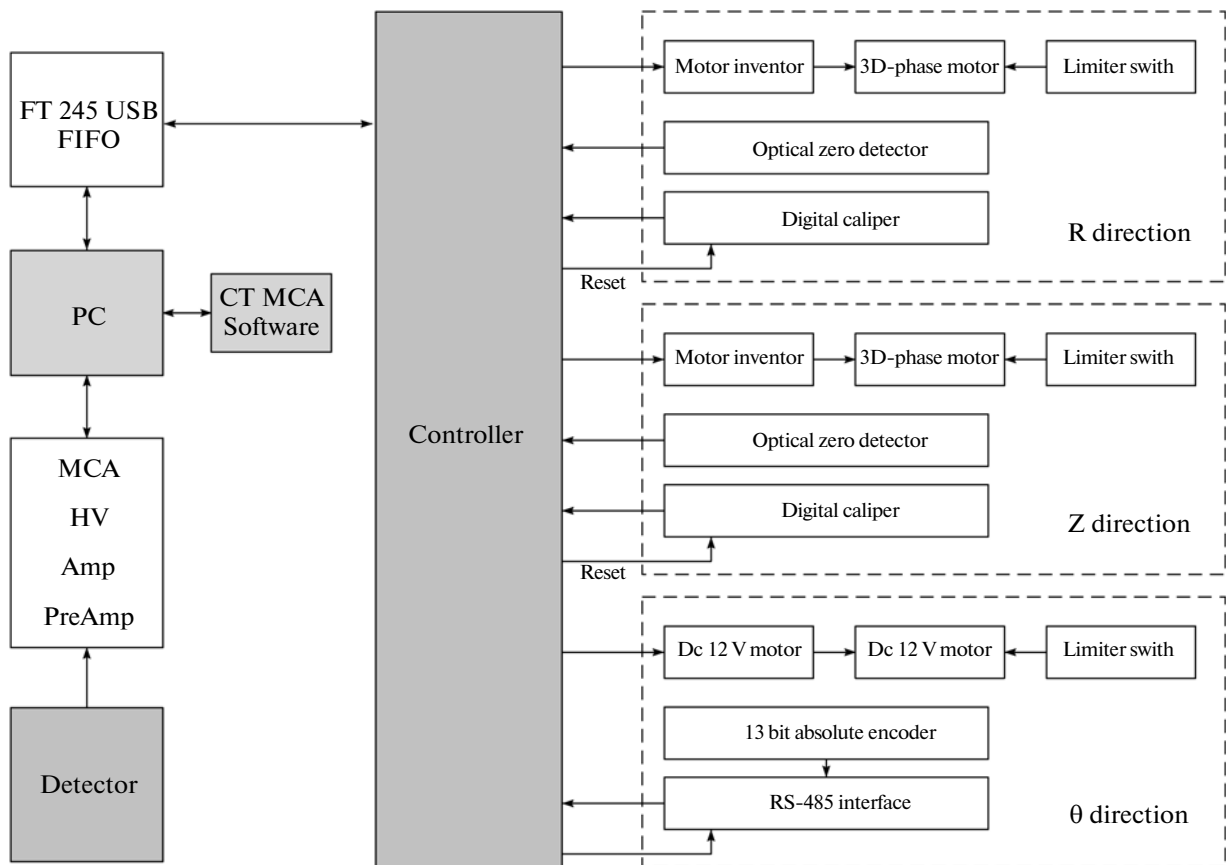


Fig. 4. Computed tomography system hardware diagram.

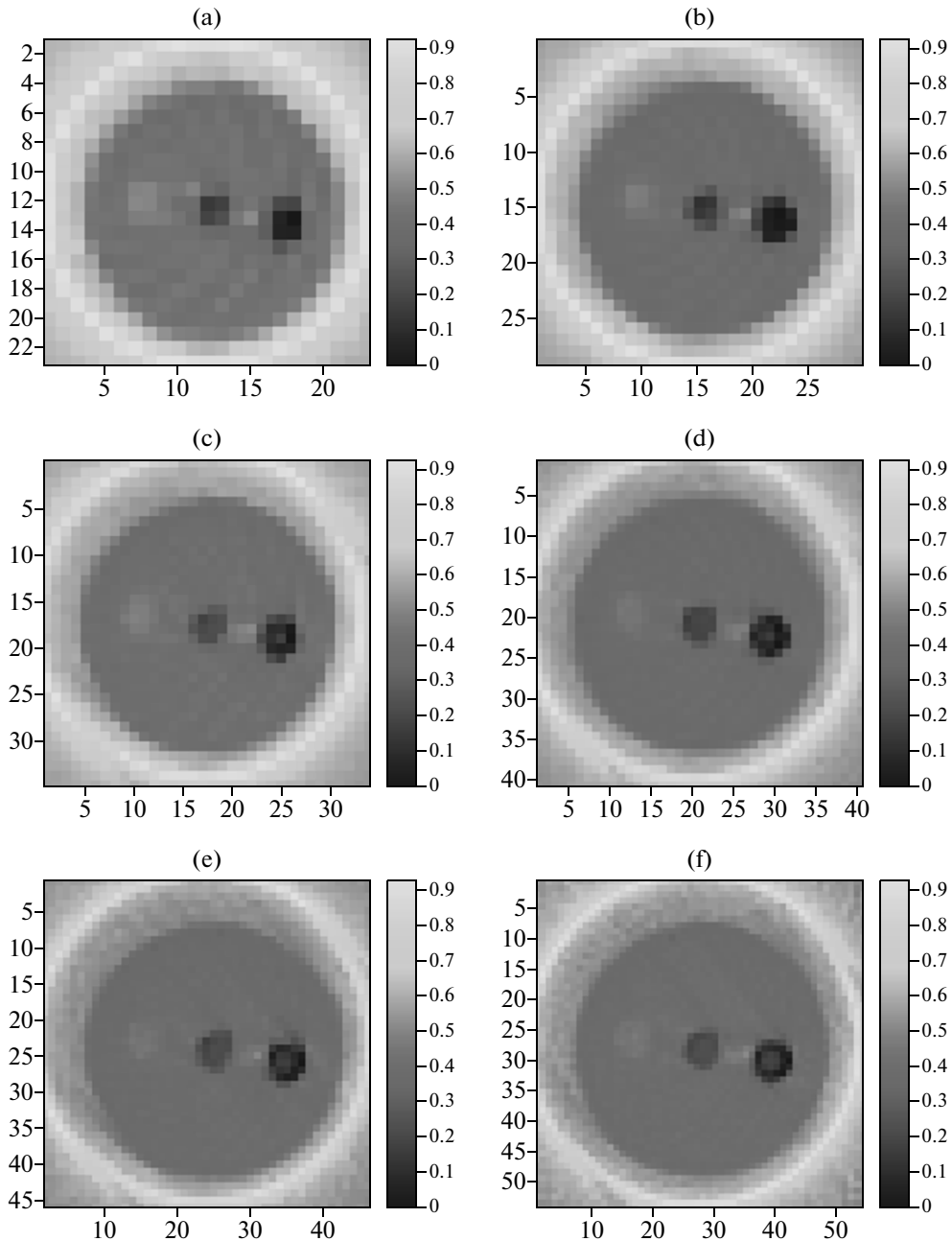


Fig. 5. Polyethylene phantom 2D-image, mercury, iron, air holes for different positions and views ($n \times m$) in each projection.

scans are taken out by scanning 180° to collect attenuation beams. There are $n \times m$ projections for producing of image and time of each projection is selected to be 3 s. The field of view (FOV) linear course is 145 mm that means 22 mm before and after of phantom.

A polyethylene phantom ($0.93 \text{ g} \cdot \text{cm}^{-3}$) is used to determine the 2D-imaging quality of the designed industrial CT system. The phantom is made as cylinder (100 mm in diameter) on which 3 holes of 15 mm in diameter are drilled. The holes are filled with expand-

ed range of density as mercury ($13.53 \text{ g} \cdot \text{cm}^{-3}$), iron ($7.874 \text{ g} \cdot \text{cm}^{-3}$) and air ($1.184 \text{ mg} \cdot \text{cm}^{-3}$) (Fig. 5).

Nuclear electronic system consists of a NaI(Tl) ($2 \times 2"$, 905-3 model, Eberline company), and a specialized MCA (PSS-1, NSTRI, Tehran, Iran) consists of pre-amplifier, amplifier, high voltage (HV) and a data acquisition system. In this MCA, universal written software can simultaneously read positions and steps, control the motors and MCA. After that, the image is reconstructed from the measured projections

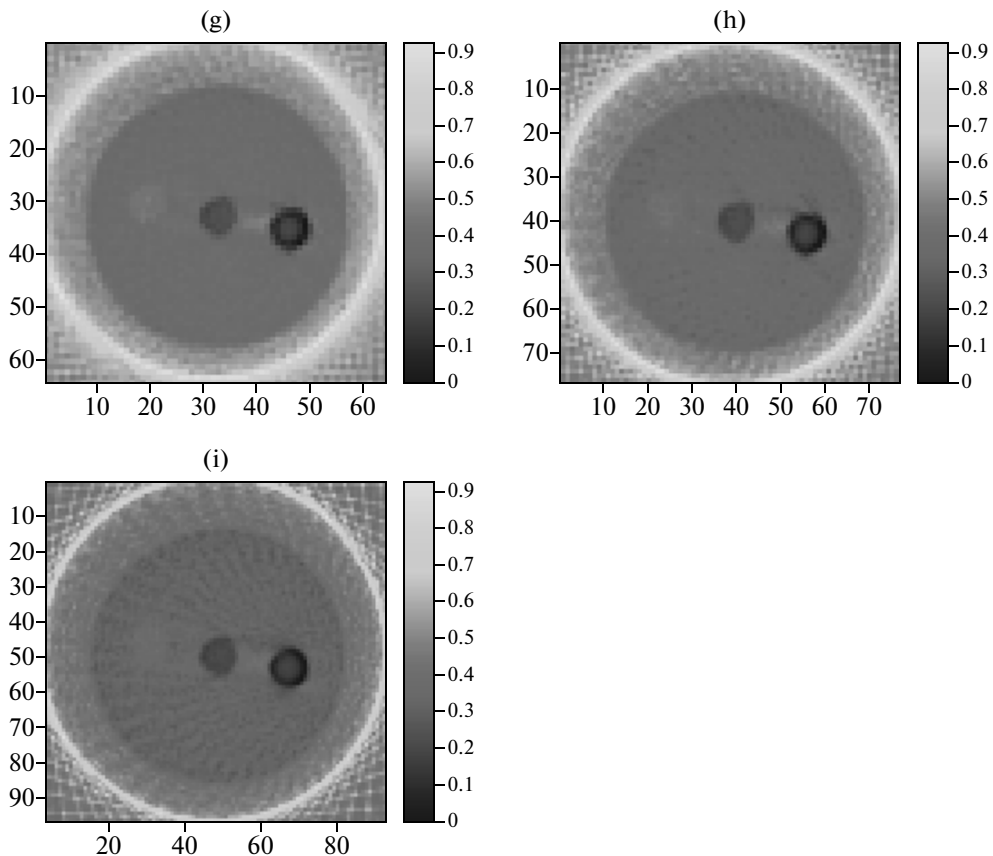
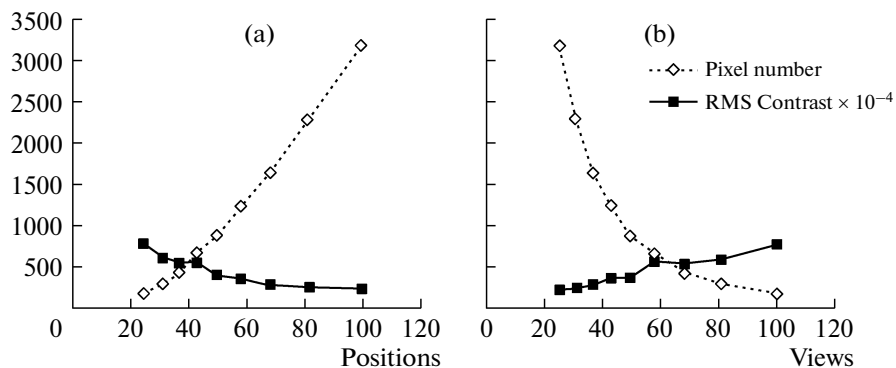


Fig. 5. Contd.

Fig. 6. The results of RMS contrast and number of reconstructed image pixels vs. (a) number of Δr (position) (b) number of $\Delta\theta$ (views).

by the filtered back projection method to bring about the inverse Radon transformation.

4. RESULTS AND DISCUSSION

Measurements are made with a source of ^{75}Se (40 mCi) and with the phantom with 3 holes. The results are represented using reconstructed images con-

sisting of the RMS contrast. In this research, experimental conditions for improving contrast such as different view and position for each projection were performed in different study cases which images were represented in Fig. 5. Also, experimental conditions, the RMS contrast and number of reconstructed image pixels for obtained results with different view and position are given in table.

Fig. 5	Δr , mm	$\Delta\theta$, °	Projection ($n \times m$)	Pixel number	RMS contrast, 10^{-4}
(a)	5.80	1.80	$25 \times 100 = 2500$	193	793
(b)	4.68	2.25	$31 \times 81 = 2511$	305	611
(c)	3.92	2.64	$37 \times 68 = 2516$	437	553
(d)	3.37	3.12	$43 \times 58 = 2494$	679	584
(e)	2.93	3.60	$50 \times 50 = 2500$	889	403
(f)	2.50	4.04	$58 \times 43 = 2494$	1245	369
(g)	2.13	4.87	$68 \times 37 = 2516$	1649	308
(h)	1.79	5.80	$81 \times 31 = 2511$	2285	261
(i)	1.45	7.21	$100 \times 25 = 2500$	3205	233

5. CONCLUSION

In general, the changing of positions and views for constant projections affect image quality. The results show that increasing number of Δr (positions) has inverse and direct relationship with RMS contrast and number of reconstructed image pixels, respectively. Also, increasing number of Δr (positions) obtained with smaller steps causes to increase reconstructed image pixels. All of the acquired results for views (m) are in reverse (Fig. 6). Therefore, for improving reconstructed image quality in industrial and medical gamma ray CT one should optimize positions and views.

REFERENCES

- Noel J., *North Star Imag Inc. J.*, 2008, vol. 1, p. 18.
- De Oliveira Jr. J.M., Martins A.C.G., de Milito J.A., *Braz. J. Phys.*, 2004, vol. 34, p. 1020.
- IAEA-TECDOC 1589, Industrial process gamma tomography, final report of a coordinated research project 2003–2007. Austria, International Atomic Energy Agency, 2008.
- Calvo W.A.P., Hamada M.M., Sprengerl F.E., *Nukleonika*, 2009, vol. 54, p. 129.
- Camp D.C., Martz H.E., Roberson G.P., Decman D.J., Bernardi R.T., *Nucl. Instrum. and Methods A*, 2002, vol. 495, p. 69.
- Lettenbauer H., Georgi B., Weiß D., *DIR 2007. International Symposium on Digital industrial Radiology and Computed Tomography*, France, Lyon: Int, NDT, 2007.
- Braz D., Lopes R.T., da Motta L.M.G., *Appl. Radiat. Isotopes.*, 2000, vol. 53, p. 725–729.
- Gholipour-Peyvandi R., Islami Rad S.Z., Ghannadi Maragheh M., *Instrum. Exp. Tech.*, 2011, vol. 2, p. 149.
- Wu Z.H., Liu J., *Appl. Radiat. Isotops.*, 2009, vol. 67, p. 1216.
- Gholipour Peyvandi R., Islami Rad S.Z., Ghannadi Maragheh M., *Int. J. Pure. Ap. Phys.*, 2010, vol. 6, p. 447–456.
- Vasquez P.A.S., de Mesquita C.H., Hamada M.M., *International Nuclear Atlantic Conference – INAC 2007*, Brazil, Santos, 2007.
- Kim J., Jung S., *Nucl. Engin. Tech.*, 2006, vol. 38, p. 38.
- Peli E., *Optic Society of America*, 1990, vol. 7, p. 2032.
- Herman G.T., *Image Reconstruction from Projections*, ed. 1, London: Academic Press, 1980.
- Herman G.T., *Fundamentals of Computerized Tomography: Image Reconstruction from Projections*, ed. 2, USA, N.Y.: Springer, 2009.
- Bushberg J.T., Seibert A., Leidholdt E.M., Boone J.M., *The Essential Physics of Medical Imaging*, ed. 2. USA, Philadelphia: Lippincott Williams & Wilkins, 2000.
- Deans S.R., *The Radon Transform and Some of Its Applications*, USA, N.Y., John Wiley & Sons, 1983.